Catalog of Large-Scale Solar Wind Phenomena during 1976–2000

Yu. I. Yermolaev, N. S. Nikolaeva, I. G. Lodkina, and M. Yu. Yermolaev

Space Research Institute, Russian Academy of Sciences, Profsoyuznaya ul. 84/32, Moscow 117997, Russia
E-mail: yermol@iki.rssi.ru
Received December 27, 2007

Abstract—The main goal of this paper is to compile a catalog of large-scale phenomena in the solar wind over the observation period of 1976–2000 using the measurement data presented in the OMNI database. This work included several stages. At first the original OMNI database was supplemented by certain key parameters of the solar wind that determine the type of the solar wind stream. The following parameters belong to this group: the plasma ratio β, thermal (NkT) and kinetic (mNV^2) pressures of the solar wind, the ratio T/T_{exp} of measured and expected temperatures, gradients of the plasma velocity and density, and the magnetic field gradient. The results of visualization of basic plasma parameters that determine the character of the solar wind stream are presented on the website of the Space Research Institute, Moscow. Preliminary identification of basic types of the solar wind stream (FAST and SLOW streams, Heliospheric Current Sheet (HCS), Corotating Interaction Region (CIR), EJECTA (or Interplanetary Coronal Mass Ejections), Magnetic Cloud (MC), SHEATH (compression region before EJECTA/MC), rarified region RARE, and interplanetary shock wave IS) had been made with the help of a preliminary identification program using the preset threshold criteria for plasma and interplanetary magnetic field parameters. Final identification was done by comparison with the results of visual analysis of the solar wind data. In conclusion, histograms of distributions and statistical characteristics are presented for some parameters of various large-scale types of the solar wind.

PACS: 96.50.Uv; 96.50.Qx; 94.30.Lr

DOI: 10.1134/S0010952509020014

1. INTRODUCTION

Since the advent of the space era, the solar wind has been permanently the focus of attention in numerous studies (see proceedings of regular "Solar Wind" conferences and, in particular, of the last of them, "Solar Wind-11" in 2005 [1]). Based on the scientific issues, one can conventionally classify these studies onto two types. On the one hand, the heliosphere represents a huge "laboratory setup" using which one can investigate dynamics of the solar wind magnetized plasma under various conditions. On the other hand, the solar wind is the main agent that transports disturbances from the Sun to the Earth. Therefore, without studying it one cannot solve a variety of space weather problem. It is precisely from this second standpoint that we describe the solar wind in this paper.

By now a large body of experimental and theoretical material concerning the mechanisms of disturbance transfer from the Sun to the Earth has been accumulated. However, the problem of quantitative description of the entire chain of interactions and, chiefly, the problem of forecasting the state of the Earth's magnetosphere based on the solar observations, is far from being solved (see, for example, recent papers on this topic [2, 3] and references therein). First of all, this is due to complexity of constructing a mathematical model that could describe the complex system including a chain of plasma regions (solar atmosphere, interplanetary medium, and magnetosphere), where different processes dominate. The initial and boundary conditions for these regions are as yet imperfectly understood. In addition, one needs to take into account that a part of the phenomena originate in the solar atmosphere, while another part is a result of dynamic processes in the interplanetary medium. In this situation, of great importance become the simplified approaches that describe the probability of separate typical phenomena instead of dynamics of the totality of physical parameters. Typical phenomena reveal themselves in distinctive sets of these parameters, which allows one in some cases to uncover dominant physical connections and to construct prognostic schemes for the "Sun–solar wind–geomagnetosphere system."

In spite of the fact that solar wind parameters are subject to large and fast variations, it was established experimentally that on characteristic scales of ~1 solar radius (700000 km) to ~1 AU (150000000 km) the solar wind is structured (i.e., it consists of differing regions and stream types propagating in the interplanetary space; inside them the parameters of plasma and interplanetary magnetic field vary comparatively slightly or according to certain known laws), and its structure is representative of the large-scale structure of

the solar corona. Certain types of the streams can be formed already in the interplanetary space at interactions of various types of the solar wind streams, and typical dimensions of these regions are, as a rule, somewhat smaller than typical dimensions of the solar wind streams associated with the large-scale structure of the solar corona. Detailed investigations of the large-scale streams in the solar wind and a comparative analysis of them would allow one to get information about physical processes in the solar wind and solar atmosphere under different conditions, as well as about processes of transferring disturbances from the Sun to the Earth with the help of various types of the solar wind. Therefore, in this paper we describe the catalog of large-scale types of the solar wind compiled by us and some preliminary results obtained with its help.

When the types of solar wind streams are classified, we use both available world experience and our original method [4, 5, 6]. This method allows us, using the set of parameters available in the OMNI database, to identify reliably 3 types of quasi-stationary streams of the solar wind (heliospheric current sheet, fast streams from the coronal holes, and slow streams from the coronal streamers), and 5 disturbed types (compression regions in front of incoming fast streams (CIR), and interplanetary manifestations of coronal mass ejections that can include magnetic clouds (MC) and EJECTA with the compression region SHEATH preceding them). In addition, we have included into our catalog such events (rare enough) as direct and reverse shock waves, and the rarefaction region RARE. Unlike CIR and SHEATH, in this case in front of MC/EJECTA a slow stream in observed after a fast stream (however, at the present stage, we do not isolate subclasses RARE after the fast stream or after a fast MC/EJECTA). All these types of the solar wind are used most frequently in the studies of similar nature, and they are described below (see Section 2.1) in more detail. It should be noted that there also exist more elaborated systems of classification of the solar wind types, including larger numbers of the types (see, for example, [7, 8] and references therein), however, we restricted ourselves to a minimum of phenomena that are usually considered in studies on solar-terrestrial physics.

To create such catalogs is an extremely important stage of these studies into solar-terrestrial physics (see, for example, the catalog of magnetic clouds (MC) according to the data of the *WIND* satellite http://lempfi.gsfc.nasa.gov/mfi/mag_cloud_publ.hmtl, http://star.mpae.gwdg.de/cme_effects/, and the ISTP Solar Wind Catalog on the website http://www-spof.gsfc.nasa.gov/scripts/sw-cat/Catalog_events.html or the Belgian catalog http://sidc.oma.be/cactus/ of solar events CME (coronal mass ejections) made using the images of the *SOHO* coronagraph http://lasco-www.nri.navy.mil/, and their manifestations in the interplanetary medium), since different types of solar wind streams are characterized by differing extent of action upon the magnetosphere or geoeffectiveness [2, 3, 6, 9–12]. However, the

approaches existing at the moment have the following drawbacks.

1. Only separate chains of phenomena are analyzed (for example, only coronal mass ejections and their manifestations in the interplanetary medium [13, 14] or only CIR [12]).

2. Not continuous series of the solar wind are studied, but only those interplanetary phenomena which are either consequences of some events on the Sun or causes of some disturbances in the magnetosphere (see, for example, [3] and references therein).

3. The roles played by all types of the solar wind in solar-terrestrial links are not compared between themselves.

4. The phenomena under consideration have small statistics, and their time series are short.

We have tried to eliminate these drawback in our catalog which was compiled starting in 2000 and underwent some changes and extension based on acquired data and new experience (some important results [6, 15–18] were obtained using a prototype of this catalog). We hope that this catalog in its present form (including the digital version ftp://ftp.iki.rssi.ru/omni/) can, on the one hand, help our colleagues in studying solar-terrestrial links. On the other hand, it can be extended and improved by our joint efforts. Some suggestions on further development of the catalog are given at the end of this paper.

2. DESCRIPTION OF METHOD

This description includes three basis sections: (1) a review of published data with substantiation of the solar wind types whose inclusion into our catalog is necessary, (2) a description of the initial database OMNI, calculations of new parameters and their inclusion into an extended database, and visualization of the data, and (3) computer and visual selection of the data according to the solar wind types.

2.1. Adopted Classification of the Solar Wind Types. It has been shown by numerous investigations that basic types of large-scale streams of the solar wind can be conventionally divided in quasi-stationary and disturbed plasma streams [19–24]. Figure 1 illustrates 6 types of the solar wind streams (some of them with sub-types), three of which (HCS, SLOW, and FAST) belong to quasi-stationary events, and three types with their sub-types (CIR/SHEATH, MC/EJECTA, and RARE) are disturbed streams.

The following streams of the solar wind can qualified as quasi-stationary: the Heliospheric Current Sheet (HCS) related to the sector structure of the solar wind and dividing regions with solar and anti-solar directions of the IMF [12, 25, 26]; the SLOW plasma stream observed above the equatorial streamer belt; and FAST plasma stream above coronal holes in which open magnetic lines dominate [27–31] (see types (1), (2), and (3) in Fig. 1). In addition to simultaneous reversals of B_X

and B_Y components of the magnetic field, the HCS event is characterized by observation of cold plasma with low velocity and high density, as well as by reduced magnetic field strength. There is no sharp boundary between the SLOW stream of the solar wind and the FAST plasma stream, just as there is no sharp boundary in topology of the coronal magnetic field when one goes over from the regions with low divergence of magnetic field lines to the regions with open field lines. Therefore, the demarcation line between the SLOW and FAST solar wind streams can be drawn conventionally. For example, we considered fluxes with velocities $V < 450$ km/s as SLOW plasma, while the solar wind with velocity $V \geq 450$ km/s was classified as FAST. It is worthwhile to note that the SLOW plasma stream represents denser and colder solar wind than hot and rarefied high-velocity FAST stream [31, 32].

Large-scale disturbances of the solar wind can be associated both with large-scale disturbances on the Sun and with disturbances originating in the interplanetary space. The phenomena originally known as "piston" belong to the first type. Later they have been associated with Coronal Mass Ejections (CME): magnetic clouds (MC) and EJECTA (or interplanetary coronal mass ejections, ICME) [11, 12, 33–41] (see Fig. 1, type (5) of streams). The magnetic fields of MC and EJECTA events have the form of a rope, and magnetic pressure dominates over thermal pressure inside them ($\beta \ll 1$). Strictly speaking, MC is a subclass of EJECTA, being distinct by stronger and more regular magnetic field, in this case observation differences can be associated both with the intensity of CME on the Sun and with the trajectory of a spacecraft relative to the magnetic rope axis in MC/EJECTA [33, 37–39, 42]. There are at least two reasons for selection of MC into a separate class: (1) historically, due to instrumental limitations in sensitivity, precisely the strongest EJECTA, i.e., MC, were first identified in the solar wind and juxtaposed with CME; (2) the strongest magnetic storms on the Earth are associated with MC. Although distinctions between MC and EJECTA are sufficiently relative (MC have stronger and more regular magnetic field than EJECTA), according to tradition we have selected a subclass MC from EJECTA and consider it separately [33, 34, 37, 42].

If a large-scale plasma volume with frozen-in magnetic field overtakes a slower plasma volume, then a compression region is formed on their boundary where plasma has increased values of density, temperature, and field strength, and $\beta > 1$. Such a scenario is realized in the solar wind in two cases. (1) When a faster MC/EJECTA moves in a slower solar wind, a compression region called SHEATH is formed before it, and under certain conditions an interplanetary shock wave can be formed on the leading edge of SHEATH [9, 43, 44] (that is, the SHEATH region often accompanies the MC/EJECTA event). (2) The fast solar wind stream can play the role of a piston, if there is a sufficiently large velocity gradient (dV/dt). In this case a region is formed
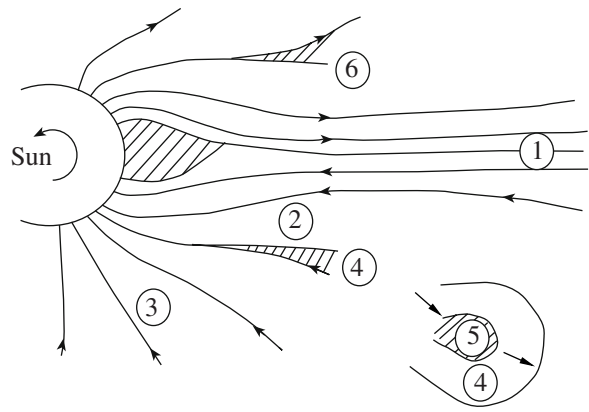

Fig. 1. Schematic representation of large-scale types of the solar wind. Digits designate (1) heliospheric current sheet (HCS), (2) slow streams from coronal streamers (SLOW), (3) fast streams from coronal holes (FAST), (4) compressed plasma (CIR on the front of fast and slow streams, and SHEATH before the leading edge of a "piston"), (5) "pistons" (magnetic cloud (MC) and EJECTA pistons), and (6) rarefied plasma on the front of slow and fast solar wind streams (RARE).

that has become known as Corotating Interaction Region (CIR) because of the fact that fast streams are formed, as a rule, in long-living coronal holes and demonstrate co-rotation with the Sun, appearing with a periodicity of solar rotation (27 days) [10, 45] (see Fig. 1, type (4)). Thought the general principle of formation is identical for SHEATH and CIR, they differ not only in the form of "pistons" forming them, but in some observational facts as well [46–48]. In view of the fact that, unlike MC/EJECTA, CIR boundary between the fast and slow streams is tilted at a small angle to the radial direction, a certain internal structure of CIR is observed at the Earth's orbit (in particular, at first an increase in density and field strength is observed and only later an increase in temperature [12]). For SHEATH events these increases are observed almost simultaneously. However, in our catalog we present the entire interaction region as CIR, without marking out finer substructures (like density increases distinctly from temperature increases).

An opposite situation is also possible in the solar wind, when fast plasma volume goes away from slow volume. In this case, a rarefaction region RARE is observed with $N < 1$ cm^{-3} [49, 50] (see type (6) in Fig. 1). As in the case of SHEATH and CIR, two types of events are possible for a volume producing rarefactions: the fast solar wind stream and MC/EJECTA, but we did not come to divide this type into two subclasses in our catalog, because of poor statistics and small geoeffectiveness of RARE.

We have included in our catalog of large-scale phenomena of the solar wind such small-scale events as the forward and backward interplanetary shock waves IS and ISA [10, 36, 51–53]. The typical time of observation of a shock wave front is of order of one minute, and
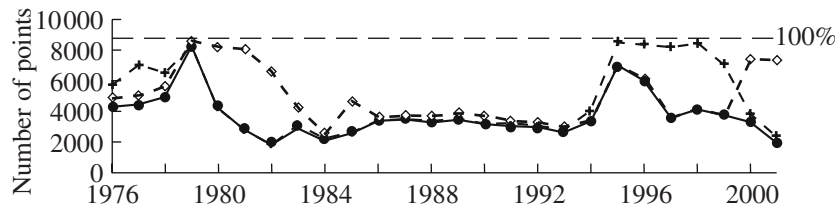
Fig. 2. Annular distributions of the number of hourly data with simultaneous measurements of three parameters (N, V, T) of plasma (crosses), magnitude and three components (B, B_X, B_Y, and B_Z) of the magnetic field (diamonds), and all seven parameters (three parameters of plasma and four of magnetic fields) (points) for the period 1976–2002 over the OMNI database. The horizontal dashed line show the maximum 100% level of data in a year.

when mean hourly values are used in the database, in most cases it is impossible to identify these boundaries (the more so, to check the validity of the Rankine–Hugoniot relations on them). Nevertheless, we have made this analysis, since interplanetary shock waves are natural boundaries of the large-scale types SHEATH and CIR, and they are frequently used when the solar-terrestrial links are studied.

Thus, a decision was made to include eight types of large-scale stream of the solar wind plasma into our catalog: HCS, SLOW, FAST, CIR, SHEATH, EJECTA, MC, and RARE, as well as two short events suspected to be IS shock and ISA inverse shock.

2.2. Calculation and Extension of the OMNI Database. The OMNI database (http://omni-web.gsfc.nasa.gov) [54] was used as original data for determination of the types of solar wind streams. It includes near-terrestrial data obtained by various satellites in the observation period from 1963 to 2001. The database represents a compilation of the magnetic field data (GSE and GSM), plasma data (densities, velocities, and temperatures of plasmas), fluxes of energetic particles, as well as certain solar indices (sunspot number) and geomagnetic indices (K_p, D_{st}, and $C9$ indices) with one-hour averaging. A more detailed description of the database is given on the website ftp://nssdcftp.gsfc.nasa.gov/spacecraft_data/omni/old_hourly/ow_data.html [54].

The original OMNI database was preliminary supplemented by the following calculated parameters of the solar wind, which are the key parameters for identification of the types of solar wind streams.

1) The ratio of thermal and magnetic pressures (beta parameter) $\beta = NkT/(B^2/8\pi)$, where N, T, and B are, respectively, density (cm^{-3}), temperature (K) of plasma (protons), and magnetic field strength (nT).

2) Expected mean temperature at expansion of the solar wind calculated based on the velocity dependence of T: $T_{exp} = (0.031V - 5.1)^2$ at $V < 500$ km/s and $T_{exp} = (0.51V - 142)$ at $V \geq 500$ km/s, where V is the solar wind velocity [55].

3) The ratio of measured and expected temperatures, T/T_{exp}.

4) Kinetic pressure of the solar wind in nPa: mNV^2, where N and V are the plasma density and velocity, respectively.

5) Thermal pressure of the solar wind in nPa: NkT, where N and T the plasma density and temperature.

6) Corrected D_{st}^* index (nT) in which there is no contribution of dynamic pressure of the solar wind: $D_{st}^* = D_{st} - 0.2(N[\text{cm}^{-3}] \times V^2[\text{km/s}])^{1/2} + 20$, where D_{st} is the usual index, and N and V are the plasma density and velocity, respectively [56, 57].

7) Increments (gradients) of density and magnetic field magnitude, DN and DB on an interval of six hours, and of velocity $DV6$ and $DV10$ on intervals six and ten hours, respectively.

It should be noted that, since the relations $T_{exp} \sim V^2 \sim 1/N$ are valid on the average, parameter T/T_{exp} turns out to be proportional to thermal pressure NkT, however, thermal pressure allows one to distinguish HCS and MC/EJECTA more reliably [2]. Nevertheless, parameter T/T_{exp} is convenient for classification of MC/EJECTA, and we have included it into the extended database and used in the analysis.

The period of observations from 1976 to 2000 was selected for compiling the catalog of large-scale events in the solar wind, since the data about the earlier period of 1963–1075 was to scanty and fragmentary. Figure 2 shows the degree of coverage of the solar wind by plasma and magnetic field data for the interval 1976–2000 according to the OMNI database. One can see in the figure that the number of simultaneous measurements of plasma and magnetic field is small (the region of simultaneous measurements of the velocity and magnetic field magnitude is equal to 48.7% of the total time in the interval under study (1976-2000)) and for some years it does not exceed 50% of time. The latter circumstance should be taken into account when comparing some yearly averaged values of some parameters, for example, the number of events per year.

2.3. Method of Data Selection. Two ways of identificated of separate stream types were used when compiling the solar wind catalog: computer identification of the solar wind types according to threshold criteria and identification by eye. To this end, a preliminary pro-

Table 1. The set of criteria used for identification of various types of solar wind streams

no.	SW type	P	N, W	V, W	B, W	T/T_{exp}, W	NkT, W	β, W	$DV6$, W	DN, W	DB, W	B_X, W	B_Y, W	T, W
1	HCS	5	>7 0.5	<500 0.5				>0.7 0.5				* **2.5**	* **2.5**	
2	SLOW	3	>3 0.5	**<450** **2.0**				<1 0.5						
3	FAST	3	<20 0.5	**≥450** **2.0**				<1 0.5						
4	CIR	5	>3 0.5		>5 0.5	>1 **3.0**	>0.007 0.5	>1 0.5						
5	EJECTA	4	<10 0.5			<0.5 **4.0**	<0.01 1.0	<0.5 1.0						
6	MC	5	<10 0.5		>10 **3.0**	<0.5 **3.0**	<0.01 1.0	<0.5 1.0						
7	RARE	4	≤1 **2.5**	<500 0.5		<1 0.5	<0.01 0.5							
8	IS	4							>50 1.0	>2 1.0	>2 1.0			**a 1.0
9	ISA	4							<−50 1.0	<−2 1.0	<−2 1.0			**b 1.0

Note: 1. HCS and IS (ISA) are boundaries rather than extended regions, therefore, for HCS * one should check reversals of B_X and B_Y components of the IMF relative to their preceding values, and for IS ** a and ISA ** b the increments of temperature $\Delta T > 0$ and $\Delta T < 0$, respectively, should be checked.
2. For SHEATH the same criteria as for CIR were used.

gram point-by-point binding of measurements to the above-listed types of streams was performed. Based on numerical criteria imposed on plasma and magnetic field parameters (see Table 1), we have estimated the probability (or the degree of reliability) that each separate one-hour point of measurement is ranked among one or another type of events. Since the time behavior of parameters is rather important (for example, CIR and SHEATH types can be distinguished only by a "piston" observed behind them: fast wind or MC/EJECTA), at the next stage we refined the kind and duration of each type of the solar wind stream identified according to threshold criteria. In addition, since we are interested in large-scale phenomena, we also smoothed to some extent small-scale variations of both measurements results and results of identification according to the threshold criteria.

As a result of such a processing, we have created an archive of graphical data of extended OMNI database including the figures with key parameters specified above over the time period 1976–2000. Figure 3 presents an example of visualization of the key solar wind parameters in the period from April 23, 1989 to April 30, 1989 (panels *1–7*) and of the results of identification of the streams according to specified criteria taking into account the weights presented in Table 1 (panel *8* in Fig. 3). (Figure 3 represents a black-white variant of color plots taken from the SRI web pages ftp://ftp.iki.rssi.ru/pub/omni/. and

ftp://ftp.iki.rssi.ru/pub/omni/catalog/. Therefore, it is less pictorial than its originals, and we recommend to look at the Internet data.) As is seen in Fig. 3 (panel *8*), first propagates the EJECTA type wind which then goes over into the CIR type. The reliability of identification of these type of events using the threshold criteria is close to unity. An interaction of the two types of events, EJECTA and CIR, is observed. During the EJECTA event, a weak magnetic storm with $D_{st} < -50$ nT is observed, while the CIR event has caused stronger magnetic storm with $D_{st} < -150$ nT (Fig. 3, panel *7*). After the CIR type, changes in the wind parameters are not significant, and their values do not correspond to the criteria of disturbed types of events. In this case, the solar wind interval following CIR is estimated according to the velocity criterion and classified as the fast solar wind (FAST). Thus, according to solar wind parameters this time interval can be attributed to two types of events at once (with different reliability): first EJECTA on the SLOW background, then CIR on the background of transition between SLOW and FAST, and finally simply FAST. The archive has been resided on the Internet, SRI website ftp://ftp.iki.rssi.ru/pub/omni/. After that, thus obtained archive of graphical data of the extended OMNI database can be used for visual identification of various types of the solar wind.
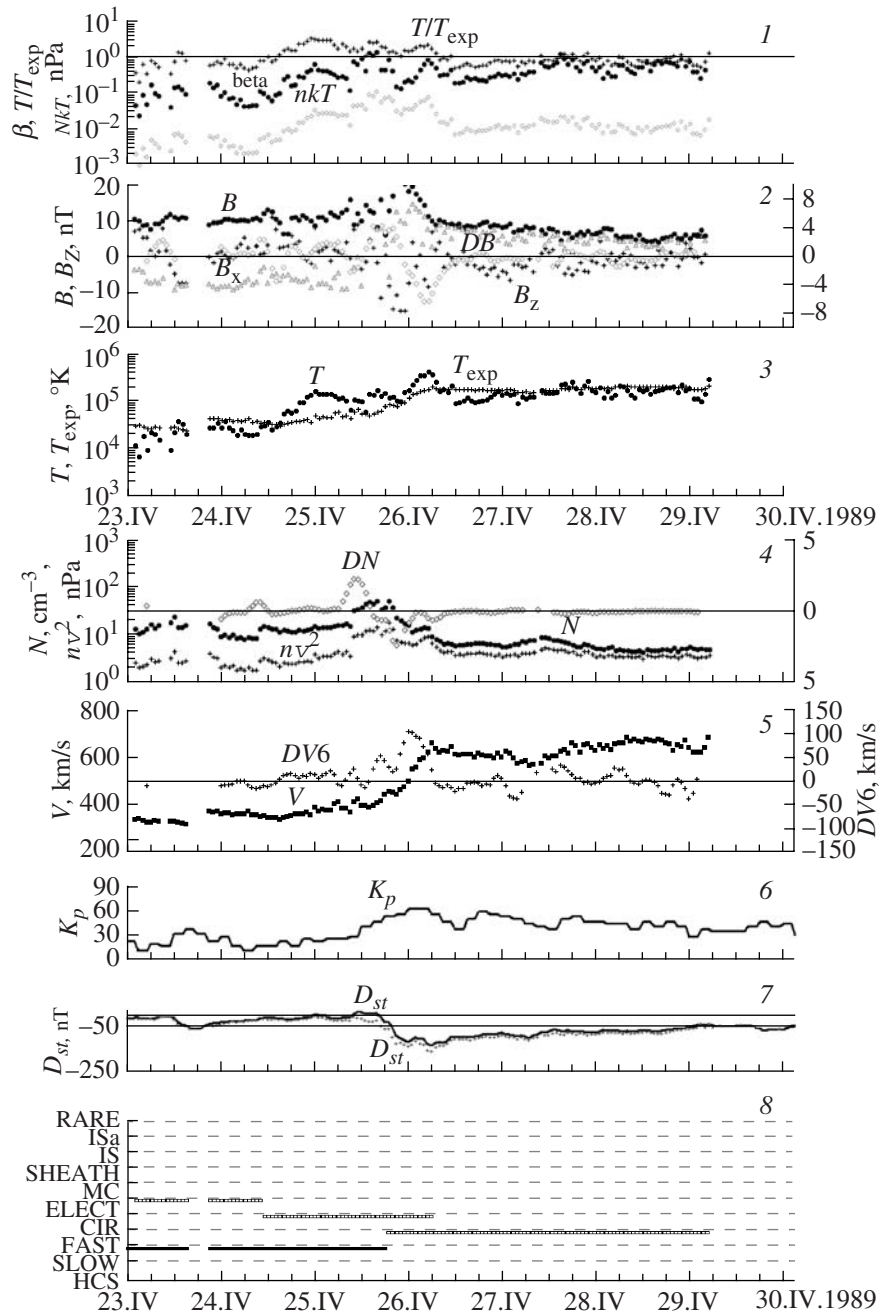
Fig. 3. An example of visualization of key solar wind parameters of the modified OMNI database for the time interval April 23–30, 1989. From top to bottom: the first panel presents β parameter, T/T_{exp}, and NkT (nPa); the second panel shows B, B_X, B_Z, and field gradient DB (nT); T and T_{exp} (K) are given in the third panel; the fourth panel presents N (cm^{-3}), mNV^2 (nPa), and density gradient DN (cm^{-3}); the fifth panel demonstrates velocity V and its gradient $DV6$ (cm^{-3}); the sixth panel shows the K_p index; and the seventh panels presents D_{st} corrected D_{st}^* indices (nT). The last, eighth panel demonstrates identification of the solar wind types according to specified criteria (see text).

The set of criteria that are used by us in program identification of the above-listed types of the solar wind plasma stream (solar wind types) is presented in Table 1.

It follows from Table 1 that each out of nine types of the solar wind (see column 2, SW type) is characterized by its own set of parameters. The number of parameters used for identification of different types is specified in column 3 (*P*). For example, five parameters were used for identification of the heliospheric current sheet (HCS), their threshold values being presented in corresponding columns (*N*, *V*, β, B_X, B_Y). At the same time, only three parameters were used for determination of the SLOW and FAST types (*N*, *V*, β). Graphic files with the numbers of satisfied criteria for each type of events

at every point of measurements (the file type is YYYYMMDD.jpg, where YYYY is year, MM is month, and DD is day) are also presented on the SRI website: ftp://ftp.iki.rssi.ru/pub/omni/catalog/, where they are allocated in separate directories according to years, from 1976 to 2001.

In addition, inside the set used for identification of various solar wind types the contribution (significance) of each parameter to event determination can differ. Therefore, for each type we had determined the main parameter of selection criterion, to which the maximum weight was assigned (see Table 1, where the main parameter is marked out in boldface, parameter weights W for each type are presented in corresponding columns). For example, simultaneous reversal of B_X and B_Y components of the magnetic field is the main indicator of HCS (each of them has weight $W = 2.5$, see Table 1). The main criterion for SLOW and FAST is the plasma velocity $V < 450$ km/s or $V \geq 450$ km/s (weight $W = 2.5$). For rarefied plasma or the RARE event very low density is the main indicator. It is worthwhile to note that, in order to identify three type of the wind (fast wind FAST, slow wind SLOW, and rarefied wind RARE), one needs information only on plasma parameters, and no magnetic data are required at all. The ratio of temperatures T/T_{exp} was assumed to be the main indicator for CIR, EJECTA, and MC (for MC one should add the large strength of magnetic field B as well). In actual practice, parameter β is shown to be more reliable for identification of these stream types, however, in order to calculate it, one needs the parameters of both plasma and field. Therefore, β is absent in the database more frequently than T/T_{exp}, and due to this reason the latter parameter was selected as a main parameter for the analysis on this stage. For interplanetary shock waves (events IS and ISA) representing the boundaries, it is necessary to satisfy all four conditions simultaneously (i.e., contributions of all four parameters to the selection criterion of these events are identical, in other words, their weights are equal). It should be noted that in case, when no magnetic data were available, for identification of the CIR, EJECTA, MC, IS, and ISA types whose criteria include the magnetic field, only plasma data were used, though such identification had lower reliability.

Thus, in order to determine to which type of the solar wind every measurement point belongs and with what probability, we calculated the ratio of the number of met criteria (taking weights into account) to their total number, also taking weights into account (see Table 1). The obtained ratio varies from 0 (if none of the criteria presented in Table 1 is met) to 1 (if all threshold criteria for a given event type are satisfied). Thus, one can assume that all measurement points having the sum of relative weights above a certain threshold value W_p (possibly different for every type of events) belong to a given stream type with a probability exceeding some threshold value. After a preliminary analysis the threshold values $W_p \geq 0.6$ were used for selecting various type of events excluding events IS (and ISA), for which it was assumed $W_p \geq 0.75$, since all conditions should be met in this case ($W_p = 1$ when magnetic field data are available, and $W_p = 0.75$ if there are no field data and only plasma data are used).

A preliminary analysis shows that for six types of the wind (HCS, SLOW, FAST, CIR, EJECTA, and RARE) selection of points with the threshold weight $W_p \geq 0.6$ means that those points are classified as a given type for which, as a minimum, the main criterion is met (while none of secondary importance criteria are met) and the points for which additional criteria (any number of them) are satisfied within the limits specified in Table 1. For the IS type the threshold value of the relative weight is $W_p \geq 0.75$. This means that only those events are selected for which either all conditions for a given type are met (when field data are available) or only plasma conditions are met (when there are no field data). Selection $W_p \geq 0.6$ for the MC type means that we select only those points at which, as a minimum, one of two main conditions (high field $B > 10$ nT or low temperature ratio $T/T_{exp} < 0.5$) is valid, and two of three secondary importance conditions (see Table 1).

As a result of processing (by program and by eye) we have got the files of point-by-point reference of the OMNI data to different types of the solar wind (see the bottom panel in Fig. 3). Namely, each point of measurements can be considered as belonging to any of nine stream types (sometimes to two types), but with different probability (degree of reliability), depending on corresponding relative total weight which was calculated for each stream type using its own numerical criteria of selection.

3. RESULTS OF ANALYSIS

In this section we present some results characterizing the behavior of various plasma and magnetic field parameters in various types of the solar wind. The total statistics (the number of intervals) of all visually identified events of different types is presented in Table 2. In so doing one should remember (see Fig. 2) that the number of annually available measurements can vary from year to year approximately twice, and it is necessary to increase the total number of events by approximately 50%. Since it is difficult to formulate the "event" concept for fast and slow streams in a physically unequivocal way, we have not included these types into those data, where events are analyzed, but they are used when parameters are determined using the number of measurements. The EJECTA and HCS events appeared most frequently, more rare were the CIR and SHEATH events, EJECTA and MC together being observed approximately twice more frequently than CIR, and only a half of them had SHEATH. Rarefied plasma RARE and reverse shock wave ISA occur least often. The number of such events per year varies

Table 2. Statistics of visually selected events (number of intervals) over the entire period 1976–2000

Type of event	Total number	Minimum number per year	Maximum number	Average number	Standard deviation
HCS	1449	17	219	57.96	46.12
CIR	884	21	55	35.4	9.04
SHEATH	740	10	51	29.6	13.9
EJECTA	1567	36	123	62.68	23.45
MC	136	0	15	5.44	4.19
RARE	18	0	8	0.72	1.8
IS	319	2	43	12.8	10.2
ISA	14	0	5	0.56	1.3

Table 3. Average values and standard deviations of parameters in various types of the solar wind during the 1976–2000 period

|	HCS	SLOW	FAST	CIR	EJECTA	MC	SHEATH	RARE
Duration, h	4.67 ± 6.05			20.6 ± 12.2	29.8 ± 20.5	28.2 ± 13.4	15.7 ± 10.1	20.1 ± 14.3
Number of events	1443			718	1127	101	642	9
N, cm^{-3}	12.1 ± 6.6	10.8 ± 7.1	6.6 ± 5.1	14.1 ± 9.9	7.8 ± 5.3	10.1 ± 8.0	14.3 ± 10.6	1.7 ± 1.8
	6208	84299	44543	12647	27259	2225	8596	139
V, 10^2 km/s	3.8 ± 0.6	3.7 ± 0.4	5.4 ± 0.8	4.5 ± 0.9	4.1 ± 0.9	4.1 ± 1.1	4.5 ± 1.1	5.1 ± 1.6
	6214	84805	44798	12666	27310	2233	8615	146
B, nT	3.9 ± 2.2	5.9 ± 2.9	6.4 ± 3.5	8.7 ± 4.1	6.4 ± 2.8	12 ± 5.2	8.5 ± 4.5	6.7 ± 2.2
	6322	67719	36179	10493	23857	2237	7286	116
$T/T_{\exp}$	0.8 ± 0.9	1.0 ± 1.4	1.0 ± 0.7	1.7 ± 2.0	0.7 ± 1.3	0.7 ± 1.5	1.5 ± 1.2	1.1 ± 0.9
	5950	75901	40026	11149	25275	2016	7851	124
T, 10^4 K	4.1 ± 4.1	4.4 ± 4.4	13.1 ± 11.8	13.8 ± 13.3	4.2 ± 5.3	4.5 ± 6.6	12.9 ± 17.6	11.1 ± 10.7
	5950	75901	40026	11149	25275	2016	7851	124
NkT, 10^{-2} nPa	0.6 ± 1.3	0.6 ± 1.3	1.3 ± 2.3	2.2 ± 2.8	0.4 ± 1.2	0.7 ± 2.0	2.2 ± 3.6	0.3 ± 0.5
	5950	75901	40026	11149	25275	2016	7851	124
β, 10^{-1}	9.5 ± 0.2	5.2 ± 0.0	6.1 ± 0.1	6.5 ± 0.1	3.1 ± 0.0	1.6 ± 0.1	6.5 ± 0.1	2.3 ± 0.5
	5878	59669	32244	8829	20518	1725	6465	100
B_Z, nT	-0.01 ± 2.3	0.08 ± 3.1	0.05 ± 3.4	0.2 ± 4.4	0.03 ± 3.3	-0.8 ± 7.7	0.10 ± 4.9	0.80 ± 2.8
	6322	67719	36179	10493	23857	2237	7286	116
D_{st}, nT	-6.5 ± 15.0	-10.7 ± 18.2	-28.7 ± 25.9	-18.0 ± 27.2	-21.1 ± 25.4	-52.1 ± 45.8	-21.5 ± 33	-27.0 ± 22.0
	6415	85459	45017	13120	29046	2571	6856	147
mNV^2, nPa	2.9 ± 1.4	2.4 ± 1.6	3.2 ± 2.8	4.4 ± 2.8	2.1 ± 1.7	3.3 ± 3.2	4.9 ± 4.7	0.8 ± 0.6
	6208	84299	44543	12647	27259	2225	8596	139

over the entire time interval under consideration, and this value can scatter by an order of magnitude (see the difference between the minimum and maximum number of events per year). For some events (for example, HCS and MC) the standard deviation relative to the mean annual number is comparable with the average value.

Numerical values characterizing the behavior of various plasma and magnetic field parameters in different types of the solar wind are presented in Table 3. The second row of the table gives average durations and their root mean square deviations for different types of the solar wind. Here and further in the table the data are presented in the form $\langle a \rangle \pm s(a)$, where $\langle a \rangle$ and $s(a)$ are the mean value and root mean square deviation of quantity a, respectively. In the second row of Table 3, below these values, the numbers of events are presented that were used for calculation of the above parameters. These numbers are somewhat lower than in Table 2, since in this case (for Table 3) we have taken only those events that had neither initial nor final intervals without
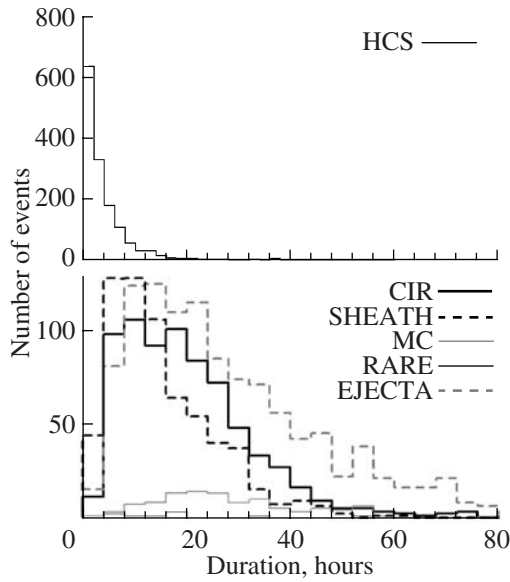
Fig. 4. Duration distributions of different types of the solar wind for the period 1976–2000.
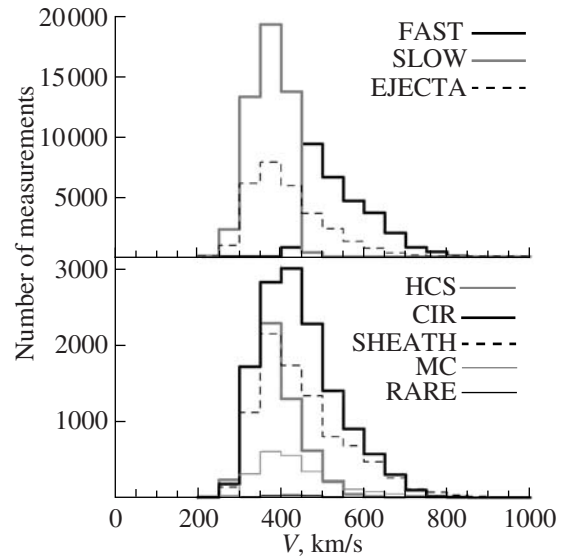
Fig. 5. The same as in Fig 4, for the solar wind velocity *V*.

plasma and magnetic field data, i.e., they were not truncated due to absence of data. These numbers turn out to be still more underestimated than in Table 2. In this case, the number of events decreases approximately proportionally to the number of events in Table 2, and it is underestimated stronger for those solar wind types that have longer duration of events. The remaining rows (after row 2) of Table 3 include the numbers of one-hour points belonging to a given type of the solar wind.

Histograms of duration distributions for events from Table 3 are presented in Fig. 4. For all types the distributions have sharp boundaries from the side of short durations and long tails in the region of long durations, which results in the fact that mean values turn out to be a bit larger than maxima of the distributions. The EJECTA and MC types whose durations are equal to 30 and 28 hours, respectively, are the longest. CIR and RARE last about 20 hours, durations of SHEATH and HCS are 16 hours and 5 hours, respectively. For the events resulted in magnetic storms [17, 18, 58] durations of EJECTA/MC and CIR turn out to be 28.3 ± 12.0 and 19.8 ± 7.7, respectively, while SHEATH events are almost twice shorter: 8.9 ± 4.7.

Below, in Figs. 5–14 we present histograms of distributions for various parameters of the solar wind plasma and magnetic field (*N*, *V*, *T*, T/T_{exp}, *NkT*, β, $mNV^2 = P_{dyn}$, *B*, B_Z) and D_{st} index for all types of solar wind streams in the time period 1976–2000.

The strongest differences in velocity (Fig. 5) are observed for FAST and SLOW solar wind streams in accordance with their definition (≥450 and < 450 km/s). For the other types of the solar wind this difference is smaller, all of them have a maximum near 400–450 km/s and long tails extending beyond 600 km/s.

Unlike velocity, density has larger variations (see Fig. 6, where the data are presented on logarithmic scale), and distinctions between various types of the streams are noticeable. The density in SLOW streams is higher than in FAST events. It is also higher in HCS, CIR, and SHEATH than in EJECTA and MC.
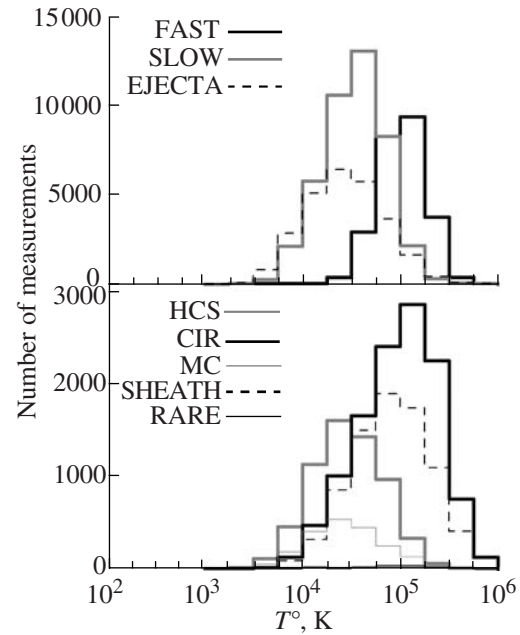
Dynamic pressure defined as a combination of squared velocity and density, mNV^2, varies in a way similar to velocity (see Fig. 7): high values are observed in fast streams FAST, CIR, and SHEATH, while low values are typical for HCS, SLOW, EJECTA, MC, and RARE.
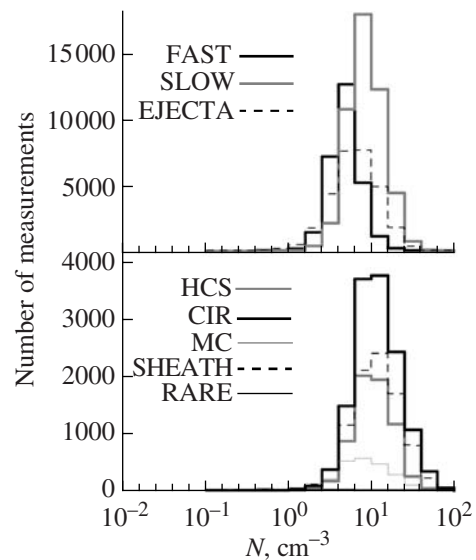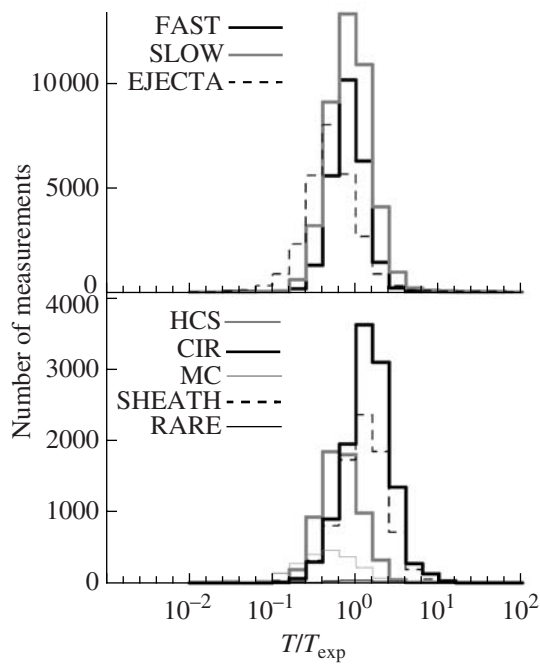

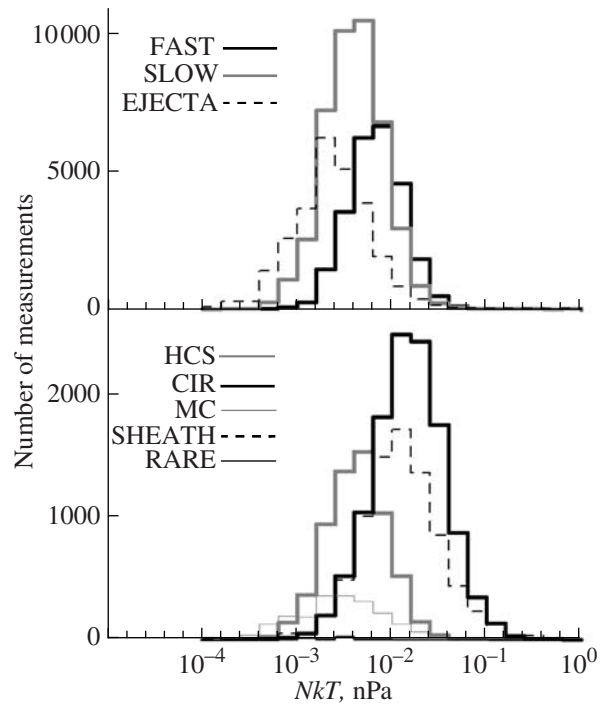**Fig. 6.** The same as in Fig 4, for the solar wind density *N*.
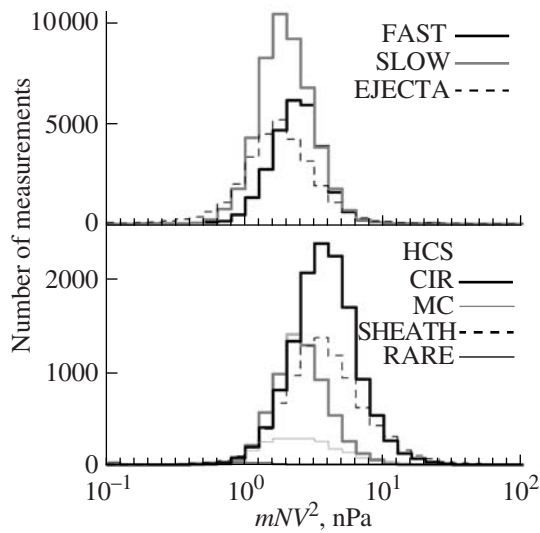
Fig. 7. The same as in Fig 4, for the solar wind dynamic pressure mNV^2.

Fig. 8. The same as in Fig 4, for the temperature of solar wind protons, T.

**Fig. 9.** The same as in Fig 4, for the relative temperature of solar wind T/T_{exp}.

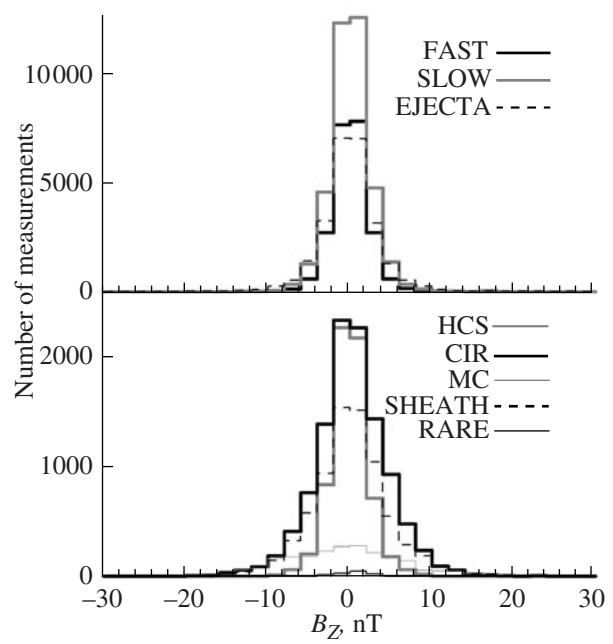**Fig. 10.** The same as in Fig 4, for the thermal pressure of the solar wind NkT.

The behavior of proton temperature (Fig. 8) is close to the velocity behavior: high temperature is observed in FAST, CIR, and SHEATH, and low temperature values take place in SLOW, EJECTA, MC, HCS, and RARE. Relative temperature T/T_{exp} (Fig. 9) is close to unity in undisturbed solar wind types FAST and SLOW,

it is higher than unity in compressed types CIR and SHEATH, and lower than unity in EJECTA, MC, HCS, and RARE.
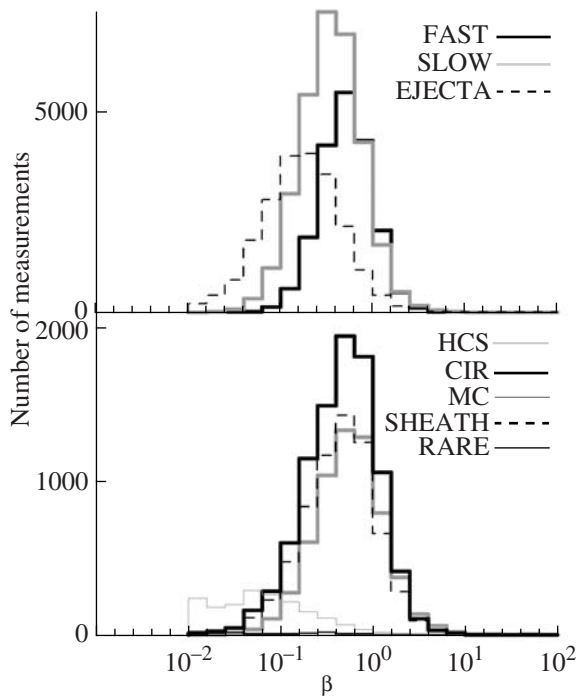
Thermal pressure of the solar wind NkT (Fig. 10) behaves itself similarly to T/T_{exp}: it is high in CIR and SHEATH, and low in EJECTA, MC, HCS, and RARE.
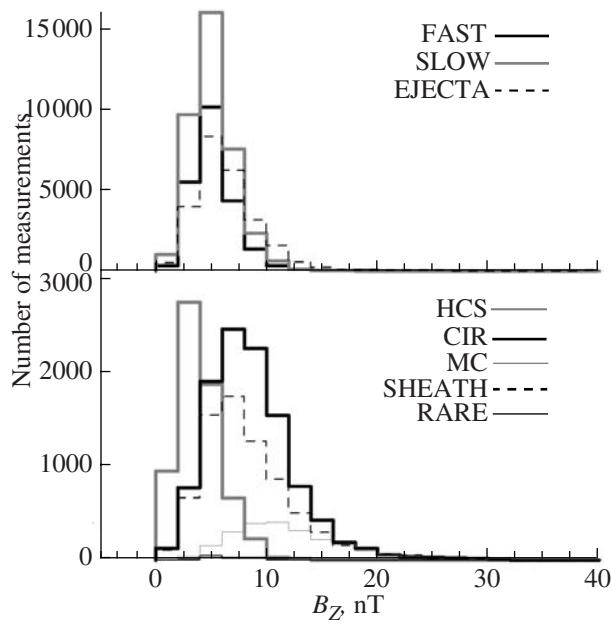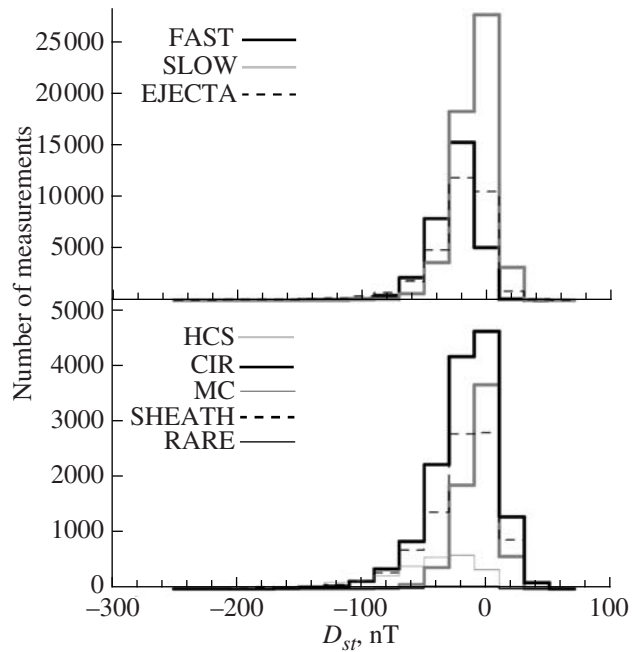
Fig. 11. The same as in Fig 4, for the interplanetary magnetic field magnitude, B.

Fig. 12. The same as in Fig 4, for the B_Z component of the interplanetary magnetic field.

Fig. 13. The same as in Fig 4, for the ratio of thermal and magnetic pressures (β parameter).

Fig. 14. The same as in Fig 4, for the D_{st} index.

The interplanetary magnetic field magnitude (Fig. 11) has high values in MC, CIR, and SHEATH, middle values are typical for FAST, SLOW, and EJECTA, and low for HCS and RARE. The IMF value is one of basic parameters for selection of MC of EJECTA. The distribution of the B_Z component of the IMF (Fig. 12) for all types of the solar wind has sufficiently symmetrical form (with equal numbers of positive and negative values), and its mean value is close to zero.

It is worthy of noting in this case that disturbed types HCS, CIR, SHEATH, MC, and EJECTA have broader distributions. This means that for them the probability of observing a noticeable south component of the IMF is higher.

The ratio of thermal and magnetic pressures (β parameter, Fig. 13) have higher values for CIR and SHEATH, and lower values for MC and EJECTA.

The D_{st} index has a maximum near the interval from 0 to –20 nT for all types of the solar wind. However, for disturbed types (having, according to Fig. 12, the broader distributions of the IMF B_Z component) CIR, SHEATH, MC, and EJECTA, and for FAST the distributions have long tails into the region of low D_{st} index values, so that the mean values turn out to be nonzero.

4. DISCUSSION ANS CONCLUSIONS

The results of our identification were partially compared to tabulated data of various events presented on the website http://star.mpae.gwdg.de/cme_effects/, and to the ISTP Solar Wind Catalog on the website http://www-spof.gsfc.nasa.gov/scripts/sw-cat/Catalog_events.html. It has been shown by preliminary analysis that strong discrepancy of the results, for example, concerning identification of the shock waves (IS) and of HCS events (up to 50%), is associated with the fact that in the catalog either magnetic field alone or field simultaneously with plasma data are absent (for example, 37 out of 47 HCS events missed by us are explained by gaps in the data). One can conclude that the main cause of the lack of coincidence is the use of different original databases. At the same time, comparison with the ISTP Solar Wind Catalog on the website http://www-spof.gsfc.nasa.gov/scripts/sw-cat/Catalog_events.html, which is compiled based on the data of satellites *WIND* and *IMP*8, demonstrates very good coincidence (95–100%) with the FAST, SLOW, and MC events. Thus, comparing our results of identification with previously obtained tables of different types of streams we have got a good agreement in more than 90% of events, some discrepancies being observed under conditions when either some parameters were not measured or complicated observed phenomenon had the features specific for several types of streams and, thus, no unequivocal interpretation was possible. For example, when two or more EJECTA/MC interact between themselves, a sufficiently complicated phenomenon comes into being. The compressed EJECTA/MC can have in this case some properties of both EJECTA/MC and SHEATH, and precisely these phenomena turn out to be heliospheric sources of the strongest magnetic storms [59]. In the future such intervals (interactions of differing stream types) apparently should be classified as separate subtypes of the solar wind streams.

Comparison of the events obtained by us with the data of other authors will be continued. Moreover, soon we hope to improve the situation considerably by using more complete OMNI2 database.

The above distributions of plasma and magnetic field parameters in various large-scale types of the solar wind clearly demonstrate that boundary values selected on the basis of numerous experiments have allowed us to make selection of all measured intervals of the solar wind and to assign each of them to a certain type (or several types, but with different degree of identification reliability). It is important to note that, unlike numerous papers where similar boundary approaches were used for selection of only one or two stream types (see, for example, [12, 13]), this paper realizes this approach with a single set of criteria to eight large-scale stream types and demonstrates that it can operate reliably. The obtained statistical characteristics and histograms of the solar wind and IMF parameters in various types of the streams well agree with previously obtained results (see [60] and references therein).

As for the plans of future development of the catalog, we would like to (1) extend it into the region of earlier observation; (2) to go over to the OMNI2 version, which would allow us to extend the catalog in the region after 2000; (3) to include into analysis the data with higher time resolution for more reliable identification of forward and backward interplanetary shock waves; and (4) to investigate the influence of thresholds on identification of rarefaction regions RARE whose selection at the moment is preformed with rather rough threshold.

REFERENCES

1. *Proceedings of the Solar Wind 11/SOHO 16 "Connecting Sun and Heliosphere" Conference (ESA SP-592) held 12–17 June 2005, Whistler, Canada*, Fleck, B., Zurbuchen, T.H., and Lacoste, H., Eds., Published by ESA Publications Division, ESTEC, Postbus 299, 2200 AG Noordwijk, The Netherlands, 2005.

2. Yermolaev, Yu.I. and Yermolaev, M.Yu., Statistic Study on the Geomagnetic Storm Effectiveness of Solar and Interplanetary Events, *Adv. Space Res.*, 2006, vol. 37, p. 1175.

3. Zhang, J., *et al.*, Solar and Interplanetary Sources of Major Geomagnetic Storms ($D_{st} < -100$ nT) during 1996–2005, *J. Geophys. Res.*, 2007, vol. 112, p. A10102. doi: 10.1029/2007JA012321.

4. Yermolaev, Yu.I., A New Approach to Studying the Large-Scale Structure of the Solar Corona Using the

Results of Measurements of Solar Wind Parameters, *Kosm. Issled.*, 1990, vol. 28, no. 6, p. 890. [Cosmic Research, p. 890].

5. Yermolaev, Yu.I., Large-Scale Structure of Solar Wind and Its Relationship with Solar Corona: *Prognoz 7* Observations, *Planet. Space Sci.*, 1991, vol. 39, no. 10, p. 1351.

6. Yermolaev, Yu.I. and Yermolaev, M.Yu., Statistical Relationship between Solar, Interplanetary, and Geomagnetospheric Disturbances, 1976–2000, *Kosm. Issled.*, 2002, vol. 40, no. 1, pp. 3–16. [Cosmic Research, pp. 1–14].

7. Ivanov, K.G., Solar Sources of Interplanetary Plasma Streams at the Earth's Orbit, *Geomagn. Aeron.*, 1996, vol. 36, no. 2, p. 19.

8. Ivanov, K.G., Arch-Filament Systems as Solar Sources of near-Earth Disturbances, *Geomagn. Aeron.*, 1996, no. 1, p. 3.

9. Zhang, J., Liemohn, M.W., Kozyra, J.U., *et al.*, A Statistical Study of the Geoeffectiveness of Magnetic Clouds during High Solar Activity Years, *J. Geophys. Res.*, 2004, vol. 109, p. A09101. doi: 10.1029/2004JA010410.

10. Echer, E., Gonsalez, W.D.., and Alves, M.V., On the Geomagnetic Effects of Solar Wind Interplanetary Magnetic Structures, *Space Weather*, 2006, vol. 4, p. S06001. doi: 10.1029/2005SW000200.

11. Koskinen, H.E.J.. and Huttunen, K.E. J., Geoeffectivity of Coronal Mass Ejections, *Space Sci. Rev.*, 2006, no. 124, p. 169. doi: 10.1007/s11214-006-9103-0.

12. Alves, M.V., Echer, E., and Gonsalez, W.D., Geoeffectiveness of Corotating Interaction Regions as Measured by D_{st} Index, *J. Geophys. Res.,* 2006, vol. 111, p. A07S05. doi: 10.1029/2005JA011379.

13. Cane, H.V. and Richardson, I.G., Interplanetary Coronal Mass Ejections in the Near-Earth Solar Wind during 1996–2002, *J. Geophys. Res.*, 2003, vol. 108, no. A4. doi: 10.1029/2002JA009817.

14. Zhang, J. Dere, K.P., *et al.*, Identification of Solar Sources of Major Geomagnetic Storms between 1996 and 2000, *Astrophys. J.*, 2003, vol. 582, p. 520.

15. Yermolaev, Yu.I. and Yermolaev, M.Yu., Statistical Relationships between Solar, Interplanetary, and Geomagnetospheric Disturbances, 1976–2000: 3,, *Kosm. Issled.*, 2003, vol. 41, no. 6, pp. 574–584. [Cosmic Research, pp. 539–549].

16. Yermolaev, Yu.I. and Yermolaev, M.Yu., Statistical Relationships between Solar, Interplanetary, and Geomagnetospheric Disturbances, 1976–2000: 2, *Kosm. Issled.*, 2003, vol. 41, no. 2, pp. 115–119. [Cosmic Research, pp. 105–109].

17. Yermolaev, Yu.I., Yermolaev, M.Yu., Lodkina, I.G., and Nikolaeva, N.S., Statistical Investigation of Heliospheric Conditions Resulting in Magnetic Storms, *Kosm. Issled.* 2007, vol. 45, no. 1, pp. 3–11. [Cosmic Research, pp. 1–8].

18. Yermolaev, Yu.I., Yermolaev, M.Yu., Lodkina, I.G., and Nikolaeva, N.S., Statistical Investigation of Heliospheric Conditions Resulting in Magnetic Storms: 2, *Kosm. Issled.,* 2007, vol. 45, no. 6, pp. 489–498. [Cosmic Research, pp. 461–470].

19. Hundhausen, A.J., *Coronal Expansion and Solar Wind*, Berlin-Heidelberg-New York: Springer, 1972.

20. Svalgaard, L., *et al.*, A Model Combining the Polar and the Sector Structured Polar Magnetic Field, *Solar Phys.*, 1974, vol. 37, p. 157.

21. Eselevich, V.G. and Fainshtein, V.G., An Investigation of the Relationship between the Magnetic Storm D_{st} Indexes and Different Types of Solar Wind Streams, *Ann. Geophys.*, 1993, vol. 11, p. 678.

22. Eselevich, V.G., *et al.*, Some Peculiarities of Solar Plasma streams from Coronal Holes, *Planet. Space Sci.*, 1990, vol. 38, p. 459.

23. Yermolaev, Yu.I. and Stupin, V.V., Helium Abundance and Dynamics in Different Types of Solar Wind Streams: The *Prognoz 7* Observations, *J. Geophys. Res.*, 1997, vol. 102, no. A2, p. 2125.

24. Goldstein, R., Neugebauer, M., and Clay, D., A Statistical Study of Coronal Mass Ejection Plasma streams, *J. Geophys. Res.*, 1998, vol. 103, no. A3, p. 4761.

25. Gonzalez, W.D., *et al.*, Interplanetary Origin of Geomagnetic Storms, *Space Sci. Rev.*, 1999, vol. 88, p. 529.

26. Tsurutani, B.T., *et al.*, Interplanetary Origin of Geomagnetic Activity in the Declining Phase of the Solar Cycle, *J. Geophys. Res.*, 1995, vol. 100, p. 21717.

27. Krieger, A.S., *et al.*, A Coronal Hole and Its Identification as the Source of High Velocity Solar Wind Stream, *Solar Phys.*, 1973, vol. 29, p. 505.

28. Burlaga, L.F., *et al.*, Sources of Magnetic Fields in Recurrent Interplanetary Streams, *J. Geophys. Res.*, 1978, vol. 83, p. 4177.

29. Sheeley, N.R. and Harvey, J.W., Coronal Holes, Solar Wind Streams, and Recurrent Geomagnetic Disturbances during 1978 and 1979, *Solar Phys.*, 1981, vol. 70, p. 237.

30. Philips, J.L., *et al.*, Ulysses at 50° South: Constant Immersion in the High Speed Solar Wind, *Geophys. Res. Lett.*, 1994, vol. 21, p. 1105.

31. Schwenn, R., Solar Wind Sources and Their Variations over the Solar Cycle, *Space Sci. Rev.,* 2006, no. 124, p. 51. doi: 10.1007/s11214-006-9099-5.

32. Schwenn, R. and Marsch, E. (Eds), *Physics of Inner Heliosphere. I*, Berlin–Heidelberg–New York: Springer, 1990, p. 99.

33. Burlaga, L.F., Sittler, E., Mariani, F., and Schwenn, R., Magnetic Loop behind an Interplanetary Shock: *Voyager, Helios*, and IMP 8 Observations, *J. Geophys. Res.*, 1981, vol. 86, p. 6673.

34. Klein, L.W. and Burlaga, L.F., Interplanetary Magnetic Clouds at 1 AU, *J. Geophys. Res.*, 1983, vol. 87, p. 613.

35. McComas, D.J., Gosling, J.T., and Bame, S.J., A Test of Magnetic Field Draping Induced B_z Perturbations ahead of Fast Coronal Mass Ejecta, *J. Geophys. Res.*, 1989, vol. 94, p. 1465.

36. Gosling, J.T., *et al.*, Coronal Mass Ejections and Large Geomagnetic Storms, *Geophys. Res. Lett.*, 1990, vol. 17, p. 901.

37. Burlaga, L.F, Magnetic Clouds, in *Physics of the Inner Heliosphere*, Schwenn, R. and Marsch, E., Eds., New York: Springer, 1991, vol. 2, p. 1.

38. Cane, H.V. and Richardson, I.G., What Caused the Large Geomagnetic Storm of November 1978?, *J. Geophys. Res.*, 1997, vol. 102, no. A8, p. 17445.

39. Blanko-Cano, X. and Bravo, S., Solar Wind Signatures Associated with Magnetic Clouds, *J. Geophys. Res.*, 2001, vol. 106, no. A3, p. 3691.

40. Schwenn, R., Dal Lago, A., Huttunen, E., and Gonsalez, W.D., The Association of Coronal Mass Ejections with Their Effects near the Earth, *Ann. Geophys.,* 2005, vol. 23, p. 1033.

41. Gopalswamy, N., Properties of Interplanetary Coronal Mass Ejections, *Space Sci. Rev.*, 2006, vol. 124, p. 145. doi: 10.1007/s11214-006-9102-1.

42. Richardson, I.G. and Cane, H.V., Regions of Abnormally Low Temperature in the Solar Wind (1965–1991) and Their Association with Ejecta, *J. Geophys. Res.*, 1995, vol. 100, no. A12, p. 23397.

43. Bravo, S. and Blanko-Cano, X., Signatures of Interplanetary Transients behind Shocks and Their Associated with Interplanetary Clouds, *Ann. Geophys.*, 1998, vol. 16, p. 359.

44. Wu, C.-C. and Lepping, R.P., Effects of Magnetic Clouds on the Occurrence of Geomagnetic Storms: The First 7 Years of Wind, *J. Geophys. Res.*, 2002, vol. 107, no. A10, p. 1314. doi: 10.1029/2001AJ000161.

45. Smith, E.J. and Wolfe, J.H., Observations of Interaction Regions and Corotating Shocks between One and Five AU: Pioneers 10 and 11, *Geophys. Res. Lett.*, 1976, vol. 3, p. 137.

46. Tsurutani, B.T., Gonsalez, W.D., Tang, E., *et al.*, Origin of Interplanetary Southward Magnetic Fields Responsible for Major Magnetic Storms near the Solar Maximum (1978–1979), *J. Geophys. Res.*, 1988, vol. 93, p. 8519.

47. Gosling, J.T. and Pizzo, V.J., Formation and Evolution of Corotating Interaction Regions and Their Three-Dimensional Structure, *Space Sci. Rev.*, 1999, vol. 89, p. 21.

48. Richardson, I.G., Cane, H.V., and Cliver, E.W., Sources of Geomagnetic Activity during Nearly Three Solar Cycles, *J. Geophys. Res.*, 2002, vol. 107, no. 8. doi: 10.1029/2001JA000504.

49. Richardson, I.G., Berdichevsky, D., *et al.*, Solar Cycle Variation of Low Density Solar Wind during More than Three Solar Cycles, *Geophys. Res. Lett.*, 2000, vol. 27, no. 23, p. 3761.

50. Yermolaev, Yu.I., Zastenker, G.N., and Nikolaeva, N.S., The Earth's Magnetosphere Response to Solar Wind Events according to the INTERBALL Project Data, *Kosm. Issled.*, 2000, vol. 38, no. 6, p. 563–576. [Cosmic Research, pp. 527–539].

51. Sonett, C.P. and Colburn, D.S., The SI+ – SI– Pair and Interplanetary Forward Reverse Shock Ensemble, *Plan. Space Sci.*, 1965, vol. 13, p. 675.

52. Richardson, I.G. and Cane, H.V., Signatures of Shock Drivers in the Solar Wind and Their Dependence on the Solar Source Location, *J. Geophys. Res.*, 1993, vol. 98, no. A9, p. 15295.

53. Ho, C.M., *et al.*, A Pair of Forward and Reverse Slow-Mode Shocks Detected by Ulysses at 5 AU, *Geophys. Res. Lett.*, 1998, vol. 25, no. 14, p. 2613.

54. King, J.H. and Papitashvili, N.E., Solar Wind Spatial Scales in Comparisons of Hourly Wind and ACE Plasma and Magnetic Field Data, *J. Geophys. Res.*, 2004, vol. 110, no. A2, p. A02209. doi: 10.1029/ 2004JA010804.

55. Lopez, R.E., Solar Cycle Invariance in Solar Wind Proton Temperature Relationships, *J. Geophys. Res.*, 1987, vol. 92, p. 11189.

56. Burton, R.K., McPherron, R.L., and Russell, C.T., An Empirical Relationship between Interplanetary Conditions and D_{st}, *J. Geophys. Res.,* 1975, vol. 80, p. 4204.

57. Gonzalez, W.G., Joselyn, J.A., Kamide, Y., *et al.*, What Is a Geomagnetic Storm, *J. Geophys. Res.*, 1994, vol. 99, p. 5771.

58. Yermolaev, Yu.I., Yermolaev, M.Yu., and Lodkina, I.G., Comment on "A Statistical Comparison of Solar Wind Sources of Moderate and Intense Geomagnetic Storms at Solar Minimum and Maximum" by Zhang, J.-C., M.W. Liemohn, J.U. Kozyra, M.F. Thomsen, H.A. Elliott, and J. M. Weygand, *JGR,* 2006. http:// arXive. org/abs/physics/0603251.

59. Yermolaev, Y.I. and Yermolaev, M.Y., Comment on "Interplanetary Origin of Intense Geomagnetic Storms ($D_{st} < -100$ nT) during Solar Cycle 23" by W.D. Gonzalez *et al.*, *Geophys. Res. Lett.,* 2008. doi: 10.1029/ 2007GL030281.

60. Yermolaev, Yu.I. and Stupin, V.V., Fluxes of Energy, Momentum, and Mass from the Sun in Various Types of Solar Wind streams according to Observations by the *Prognoz-7* Satellite, *Kosm. Issled.*, 1992, vol. 30, no. 6, p. 833. [Cosmic Research, p. 672].